ACS Sustainable Chemistry & Engineering

Research Article

pubs.acs.org/journal/ascecg

Highly and Fully Water Dilutable Sustainable Microemulsions with Dibasic Esters as Oil Phase

Michael L. Klossek, Didier Touraud, and Werner Kunz*

Institute of Physical and Theoretical Chemistry, University of Regensburg, 93040 Regensburg, Germany

ABSTRACT: In this study, we show a strategy of formulating highly and fully water dilutable sustainable microemulsions with dibasic esters as oil pseudophase. First, dimethyl or diethyl DBEs with different numbers of carbon atoms between the ester functions (succinate C2, glutarate C3, and adipate C4) or DBE blends and a surfactant−cosurfactant melt consisting of sodium dodecylsulfate and 1-pentanol with a constant weight ratio of 1:2 are used. We investigated the extent of the realms of existence of homogeneous single phases and represent them with pseudoternary phase diagrams. It was possible to formulate fully water dilutable oil-rich single-phase solutions with all dimethyl dibasic esters but not with the diethyl ones. By mixing the most hydrophilic dibasic ester with the most hydrophobic one with a mass ratio of 3:2, a fully water dilutable oil-rich single phase could also be obtained. The presence of water-in-oil, bicontinuous, and oil-in-water microemulsions was checked with conductivity and dynamic light scattering measurements. A percolative behavior was observed for all systems. Second, to formulate green and sustainable microemulsions, we replaced successively sodium dodeylsulfate by sodium oleate and 1-pentanol by ethanol or 1,5-pentanediol. With sodium oleate, highly water dilutable microemulsions were obtained. Homogeneous and translucid samples in the very diluted area turned bluish after several days. Longtime pH measurements of systems containing sodium oleate showed no degradation of the dibasic esters at low water content and a rapid hydrolysis at high water content with 1-pentanol as cosurfactant. Always in presence of sodium oleate, the substitution of 1-pentanol by ethanol or 1,5-pentanediol drives the system to microemulsions showing an instability of the ester at any water concentrations. Thermal gravimetric analysis measurements at 32 °C for 24 h confirmed a rapid evaporation of ethanol and water and negligible evaporation of 1,5-pentanediol.

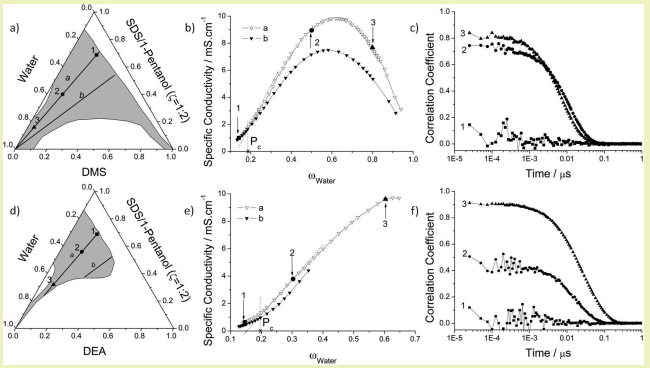

KEYWORDS: *Microemulsion, Dilutable, Dibasic ester, Ethanol, 1,5-Pentanediol*

INTRODUCTION

Solvents are an omnipresent class of chemicals. The company GlaxoSmithKline, for example, has estimated that ca. 85% of the total mass of chemicals in pharmaceutical processes are solvents, and only between 50 and 80% are recovered.[1] Because of the high quantities of solvents in our environment, the quest and need of finding and developing green alternatives are evident. Solvents should be environmentally friendly and have low costs, low toxicity, high stability, and rather high boiling temperatures. One group of solvents fulfilling most of these requirements are dibasic esters (DBEs). Moreover, they have viscosities and densities close to water. DBEs are oxygenated organic compounds of the diester type with the formula $CH_3(CH_2)_mOC(O)(CH_2)_nC(O)O(CH_2)_mCH_3$, where n is an integer and m is zero for dimethyl esters or one for diethyl esters. Starting from dibasic acids, DBEs can be synthesized via esterification with alcohols, produced in most instances from renewable feedstock, or also available from caprolactam plants in which the dibasic acids are considered waste compounds. They have excellent properties in industrial applications where especially aromatic hydrocarbons and chlorocarbons have to be replaced.[2] Many patents can be found in the fields of industrial cleaning applications,[3−6] paint,[7] coating,[7−9] and the polymer industry.[10−12] In these industries, DBEs are even recycled by vacuum distillation.[13] The diesters of succinic, glutaric, and adipic acids are the most promising DBEs in terms of green chemistry. Between 20,000 to 30,000 t/a of succinic acid, also known as amber or butanedioic acid, are produced worldwide.[14] It can be used as a precursor for many important chemicals in industry, such as N-methylpyrrolidone, 1,4-butanediol, γ-butyrolactone, adioic acid, tetrahydrofuran, and linear aliphatic esters.[15,16] Today, the starting material of succinic acid production is often liquefied petroleum gas or petroleum oil via maleic anhydrid, which has to be oxidized afterward. This last synthesis step is a serious limitation that explains why the global market and the production of maleic anhydrid is much larger than for succinic acid.[17,18]

Received: November 2, 2012
Revised: March 4, 2013
Published: April 4, 2013

In the last years, scientists have screened and studied many different microorganisms, like fungi[19,20] or bacteria,[21,22] for succinic acid production. A fermentative process using *E. coli* bacteria and a large amount of renewable feedstock, including glucose, ligno-cellulosic sugars (mixed C5 and C6), and glycerol, was scaled up by the company ARD (Pomacle, France) to 2000−3000 t/a.[23] This quantity is already around 10% of the total succinic acid production worldwide. A mentionable side effect is that CO_2 is fixed into the succinic acid during fermentation. In theory, one mole of CO_2 is needed per mole of succinate produced.

Commercial glutaric acid is a side product of the chemical adipic acid production, but glutaric acid can be obtained from bacteria as well.[24] The starting material for adipic acid is currently benzene from crude oil. Hydrogenation of benzene to produce cyclohexane is followed by air oxidation to yield a mixture of cyclohexanol and cyclohexanone.[25,26] Rennovia has recently shown a strategy to transform D-glucose from biomass to adipic acid,[27] and Verdezyne[28] has opened a pilot plant to produce adipic acid from renewable resources in Carlsbad, California. For the moment, adipic acid production by fermentation remains still "homeopathic" in front of the chemical one.

In order to reduce the quantity of solvent in a process, water can be added.[29] Moreover, the addition of water to oils leads to a higher heat capacity that is a benefit in lubricants and cutting fluids.[30] An elegant way is to transform the system into a microemulsion. Beside this aspect, very often the physicochemical properties of microemulsions are favorable as well. For example, low interfacial viscosity is important in cleaning processes and enhanced oil recovery.[30]

Microemulsions (mE) are optically transparent, thermodynamically stable, isotropic solutions[31,32] that have an extremly low interfacial tension.[33] They consist of at least a hydrophilic and hydrophobic liquid and a surfactant.[34,35] Often also a cosurfactant is needed that can be a short- or medium-chain aliphatic alcohol.[34] On the microscopic scale, mEs are structured in terms of domains of well-defined droplets (either water-in-oil (w/o) or oil-in-water (o/w))[36,37] or bicontinuous structures.[38,39] A key method of investigating the nanostructure of mEs is the measurement of the specific conductivity, κ, especially in the case of w/o mEs.[40,41] Two behaviors can be observed. The first one is a percolative behavior, where the κ value undergoes a significant change over many orders of magnitude when the volume fraction of water is increased above a certain threshold. The second one is an antipercolative behavior, where no specific change of the electrical conductivity is observed. This phenomenon can be associated with the formation of droplets with a rigid interfacial film, which prevents the reversed micelles to merge.[42]

Applications of mEs can be found in several industrial fields, e.g., degreasing agents,[43,44] cosmetic,[45,46] pharmaceutical,[47−49] food,[50,51] etc., due to their high solubilization capacity of hydrophilic and lipophilic compounds.[52] The use of DBEs in mE systems for industrial applications has already been described in several patents.[4−6,53] Until now to the best of our knowledge, no studies have shown a coherent comparison of the influence of different carbon chain lengths between the ester functions, different carbon chain lengths of the alcohol, or on the stability of the diesters against hydrolysis in the water-rich area. In this work, we focus on mEs with the dimethyl and diethyl diesters with succinic, glutaric, and adipic acids as oil pseudophase.

We present pseudoternary phase diagrams (PTPDs) and the realms of existence of mEs in the model system water/SDS/1-pentanol/DBEs, where the surfactant-to-cosurfactant mass ratio (ζ) is kept constant at 1:2. In order to make the system more sustainable, SDS is then replaced by sodium oleate and 1-pentanol by either ethanol or 1,5-pentanediol. The world production of bioethanol is estimated to be 22,000 millions of U.S. liquid gallons per year.[54] 1,5-Pentanediol can be obtained by hydrogenation of glutaric acid[55] or using furfural as the starting material.[56,57] These ways of synthesizing give the possibility to get sustainable 1,5-pentanediol from renewable feedstock. Compared to the use of ethanol, a lower vapor pressure and an increase in the boiling point of the formulations can be expected. The nanostructures of the systems were investigated with conductivity and DLS experiments, and the long-time stability of the esters was checked with pH-measurements.

EXPERIMENTAL SECTION

Materials. All dibasic esters were purchased from Sigma Aldrich (Steinheim, Germany) and have the following purities: DMS 98%, DES ≥ 99%, DMG 99%, DEG ≥ 99%, DMA ≥ 99%, and DEA 99%. Sodium oleate (purity ≥82%) and 1,5-pentanediol (≥97%) were also purchased from Sigma-Aldrich (Steinheim, Germany), ethanol (purity ≥99.9%) from Baker (Deventer, Netherlands), sodium dodecylsulphate (ultrapure) from AppliChem (Darmstadt, Germany), and 1-pentanol (≥98%) from Merck (Hohenbrunn, Germany). All chemicals were used without further purification. All solutions and microemulsions were prepared using water with a resistivity of 18 MΩ cm.

Methods and Techniques. *Phase Diagrams.* The realms of existence of mEs were determined, and pseudoternary phase diagrams (PTPDs) for the model system water/surfactant/cosurfactant/oil were established. In the first experiments, the surfactant/cosurfactant blend consisted of SDS and 1-pentanol with a constant surfactant-to-cosurfactant mass ratio of ζ = 1:2. The oil phase consisted of DBEs (dimethyl or diethyl esters of succinic, glutaric, or adipic acid) or DBE blends. To formulate more sustainable mEs, SDS was replaced by sodium oleate and 1-pentanol either by ethanol or 1,5-pentanediol, whereas ζ remained 1:2, and the oil phase was a mixture of dimethyl succinate (DMS) and diethyl adipate (DEA) with $R_{DMS/DEA}$ = 3:2. The phase diagrams were recorded using a static process according to Clausse et al.[58] In screwable tubes, blends of the emulsifying agents (surfactant and cosurfactant) were filled in the right proportions and melt with DBEs or DBE blends or water to obtain a starting weight of 3 g. Water (oil) was added successively with Eppendorf pipettes until a change in the phase behavior occurred. The phase transition was determined with the naked eye. In order to discern the homogeneous liquid crystalline (LC) phases, polarized filters were used. Under polarizing filters, most of the liquid crystalline phases appeared birefringent. Besides mEs, LC phases, "classical" emulsions, and clear homogeneous solutions in equilibrium with undissolved surfactant appeared. At the transparent-to-turbid boarder, the weight fractions of water (oil) were derived from precise weight measurements. The composition of the solution was then calculated from the masses of all components. It was estimated that the accuracy of the compositions for the transparency-to-turbidity transition was better than 2%. The temperature was kept constant at 25 °C with a thermostatically controlled test tube rack.

Conductivity. All measurements were carried out along experimental paths with a constant surfactant + cosurfactant(s)-to-oil ratio (H). This ratio is

$$H = \frac{\text{surfactant} + \text{cosurfactant (weight\%)}}{\text{DBE (weight\%)}} \quad (1)$$

The studied variable was the water mass fraction ω_{water}. For all studied systems, experimental paths *a* (H = 4) and *b* (H = 3:2) were investigated as shown in Figure 1. The starting DBE single-phase

dx.doi.org/10.1021/sc300132x | ACS Sustainable Chem. Eng. 2013, 1, 603−610

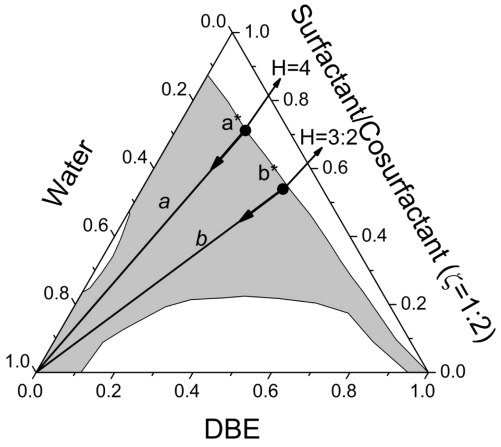

Figure 1. Representation of experimental paths *a* and *b*, starting from the compositions a* and b* in a classical PTPD. With a surfactant + cosurfactant-to-DBE ratio (H) equal to 4 (path *a*) or 3:2 (path *b*).

solutions were prepared with a water content as low as possible (compositions corresponding to points a* and b*, Figure 1). Water was then progressively added with an Eppendorf pipet and ω_{water}, and the corresponding specific conductivity κ were recorded. The direction followed during the experiments is given by the arrows in Figure 1. Conductivity measurements were carried out at 25 °C with an inoLabVario Cond 730 conductometer. The temperature was controlled by a thermostatted cell. All measurements were conducted twice. The experimental error was approximately 2.5%. The measurement was finished when the turbid area was reached. Again, the compositions were calculated from the masses of all components.

Dynamic Light Scattering. Dynamic light scattering (DLS) experiments were performed with the help of a goniometer CGS-II from ALV (Germany). The goniometer was equipped with an ALV-7004/Fast Multiple Tau digital correlator and a vertical-polarized 22mW HeNe laser (wavelength λ = 632.8 nm). All measurements were done at a scattering angle of 90° after thermostatting to 25 °C. Before the measurements, all solutions were filtered with a 0.2 μm PTFE membrane filter to remove all dust particles. Then, the samples were transferred to a cylindrical light-scattering cell with a 10 mm outer diameter. The experimental compositions were the same as those chosen for the conductivity measurements (path *a* in Figure 1).

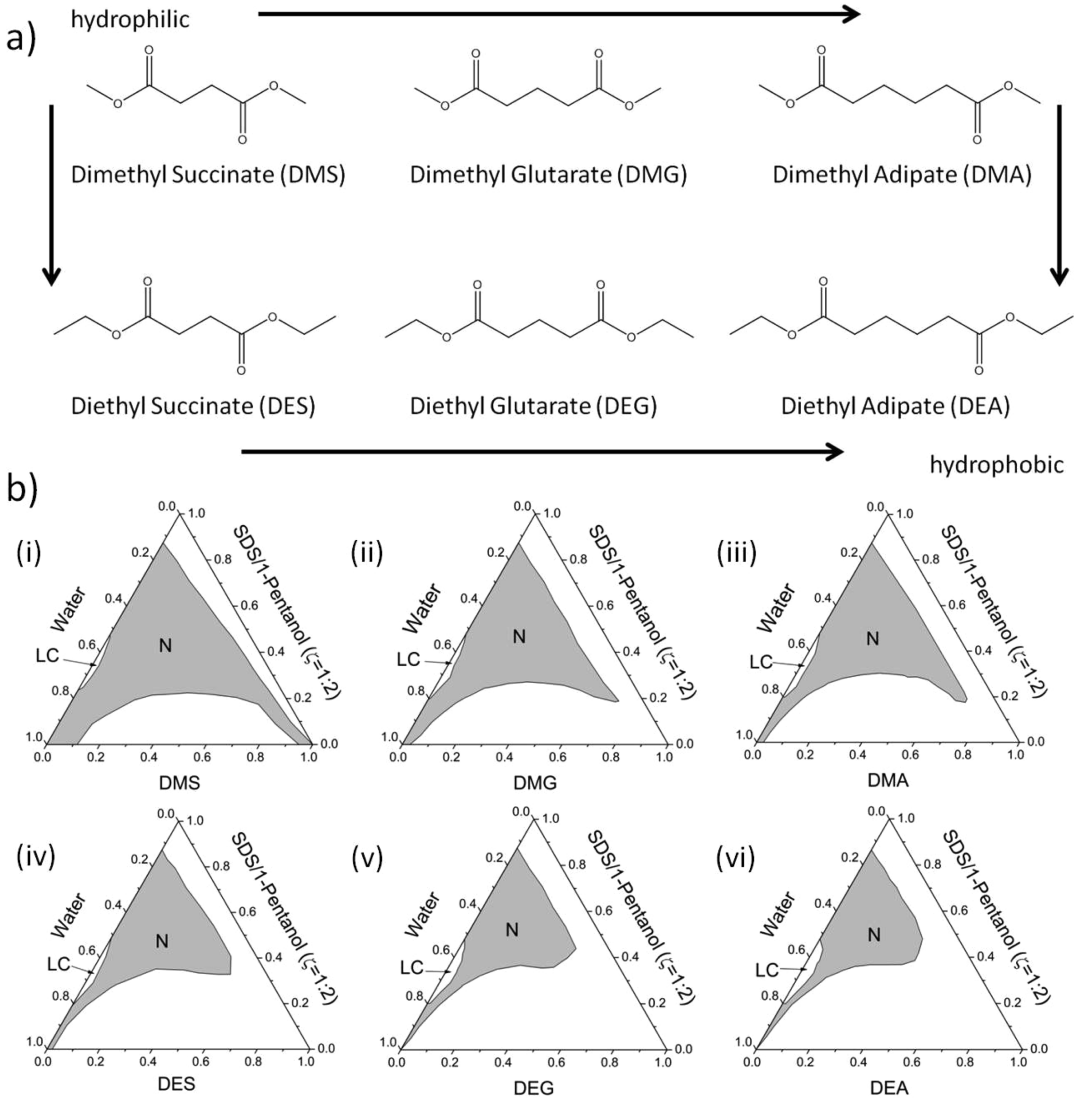

Figure 2. (a) Molecular structure of the six DBEs used in this study ordered by hydrophobicity. (b) PTPDs of the systems water/SDS/1-pentanol/(i) DMS, (ii) DMG, (iii) DMA, (iv) DES, (v) DEG, and (vi) DEA at 25 °C and with ζ = 1:2. The gray areas represent the homogeneous single-phase regions (N). All compositions are in weight ratio.

The measurement time was 300 s. We focused on the shape of the correlation functions, and we were not interested in the overall particle sizes.

Stability Experiments. DBE Stability. The stability of the DBEs in the formulations was checked with pH measurments. For this reason, selected samples with either SDS or sodium oleate as surfactant were investigated. All samples had compositions corresponding to the experimental path *a* (Figure 1). The experiments were performed with a SchottpH-meter from Nova Analytics (Weilheim, Germany) and a 601 Metrosensor-Glass-Electrode from Metrohm (Herisau, Switzerland). During the measurements, the samples were thermostatted at 25 °C with a water bath.

Thermogravimetric Analysis (TGA). The volatilities of the components in the microemulsions were investigated with thermogravimetric experiments. Samples of microemulsions of 13 mg were subjected to thermogravimetric analysis in an air atmosphere. A TGA7 instrument (Perkin-Elmer, Norwalk, CT, U.S.A.) was used. An isothermal heating program was set up at 32 °C. In order to obtain a low-noise TG signal, a constant gas flow of 45 mL/min was set for all tests. The precision of temperature measurements for the thermobalance was ±1 °C. Continuous records of weight loss and temperature were obtained and used to determine the evaporation rates (weight loss %/min). The experimental time was 24 h.

RESULTS AND DISCUSSION

Phase Diagrams with DBEs. In the first step, the phase behaviors of the system water/SDS/1-pentanol/DBE with six different DBEs, dimethyl/diethyl succinate (DMS, DES), glutarate (DMG, DEG), and adipate (DMA, DEA) were investigated. In Figure 2a, the structures of the six molecules are shown. These components differ by the number of carbon atoms between the two ester functions (succinate C2, glutarate C3, and adipate C4) and the alcohol used in the esterification process (methanol or ethanol). In this ordering, DMS is the most "hydrophilic" and DEA the most "hydrophobic" DBE. Figure 2b illustrates the resulting PTPDs of the systems water/SDS/1-pentanol/DBE. The gray areas represent the clear and homogeneous single-phase regions. All dimethyl esters form large areas of single-phase regions that are fully water dilutable. In the case of DMS, the single-phase area stretches even to the oil-rich corner, but this region was not in the field of interest of this study and was not examined in details. In contrast, the extent of the single-phase area for diethyl esters is restricted to the oil- and surfactant-rich area. They have a small channel to the water-rich zone for well-defined paths, but this type of mE is not fully water dilutable. A detailed study of the nanostructure of the systems will be given later. In all the described systems, LC phases occur near the water−surfactant binary.

As already shown in a previous work,[59] by mixing two oils, an intermediate behavior of the resulting mixture can be expected. Therefore, in the next step, the most "hydrophobic" diester, DEA, which produces only a relatively thin monophasic area in the water-rich region, is mixed with the most hydrophilic one, DMS, which gives the largest area of homogeneous single phase (Figure 2b). The "best" mixing ratio of these two DBEs is defined as a compromise of a high concentration of DEA in the melt and a high water solubility. In Figure 3a, the water solubility of this DBE melt, $\omega_{DBE,added}$, of these solutions is plotted vs the weight ratio of DMS, $R_{DMS/DEA}$, in the DBE blend. With the ratio $R_{DMS/DEA}$ = 3:2, a good solubility in water was kept. Again, a fully water-dilutable mE was obtained.

Toward Sustainable "Microemulsions". The mixture of SDS and 1-pentanol as amphiphilic pseudophase is still a drawback in the formulation of sustainable mEs. To overcome this obstacle, sodium oleate was used as alternative surfactant and ethanol or 1,5-pentanediol as cosurfactant. The components were progressively replaced for a better understanding of the influence of each ingredient on the formulation. In Figure 4, the resulting PTPDs of the systems water/sodium oleate/DMS/DEA/(a) 1-pentanol, (b) ethano, and (c) 1,5-pentanediol with $R_{DMS/DEA}$ = 3:2 and ζ = 1:2 are shown. In the system

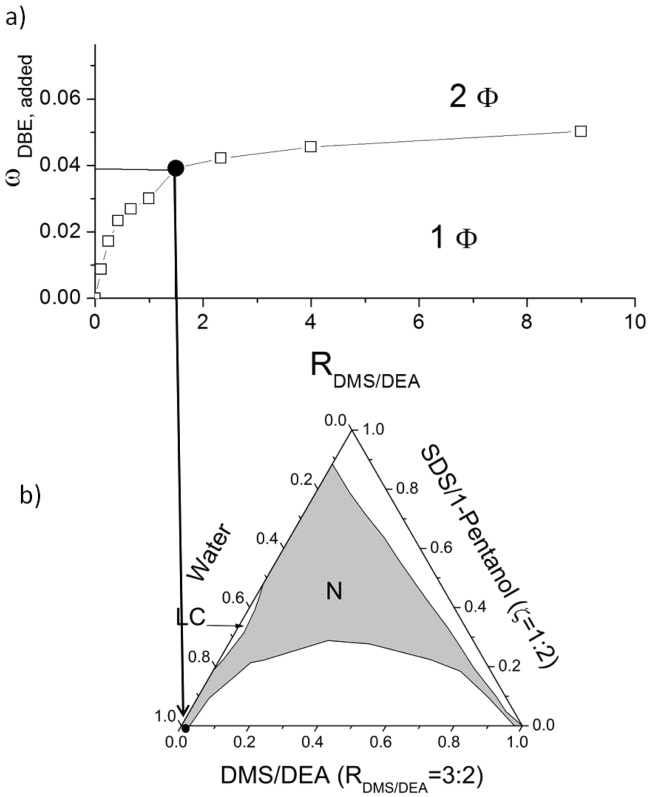

Figure 3. (a) Phase diagram of the water solubility of different DMS/DEA blends. The mass fraction of DBE blend, possible to dissolve in water, $\omega_{DBE,added}$, is plotted as a function of the weight ratio of DMS, $R_{DMS/DEA}$, in the DBE blend. (b) PTPD of the system water/SDS/1-pentanol/DMS/DEA with ζ = 1:2 and $R_{DMS/DEA}$ = 3:2 at 25 °C.

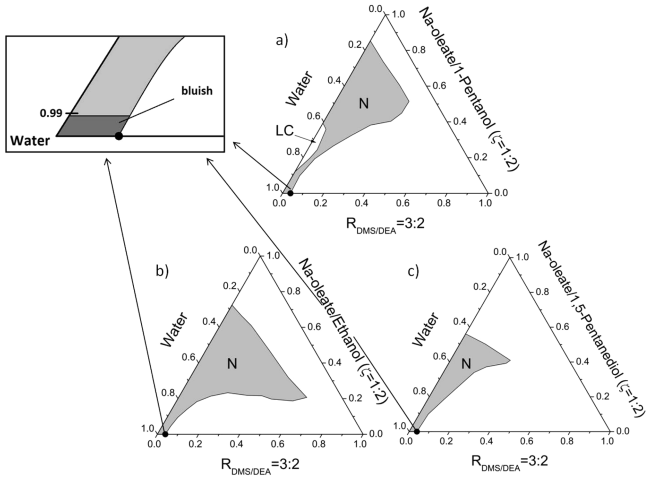

Figure 4. (a) Phase diagram of the pseudoternary system water/sodium oleate/1-pentanol/DMS/DEA with $R_{DMS/DEA}$ = 3:2 and ζ = 1:2 recorded at 25 °C. (b) In this system, 1-pentanol was replaced by ethanol, and (c) ethanol was replaced by 1,5-pentanediol.

dx.doi.org/10.1021/sc300132x | ACS Sustainable Chem. Eng. 2013, 1, 603−610

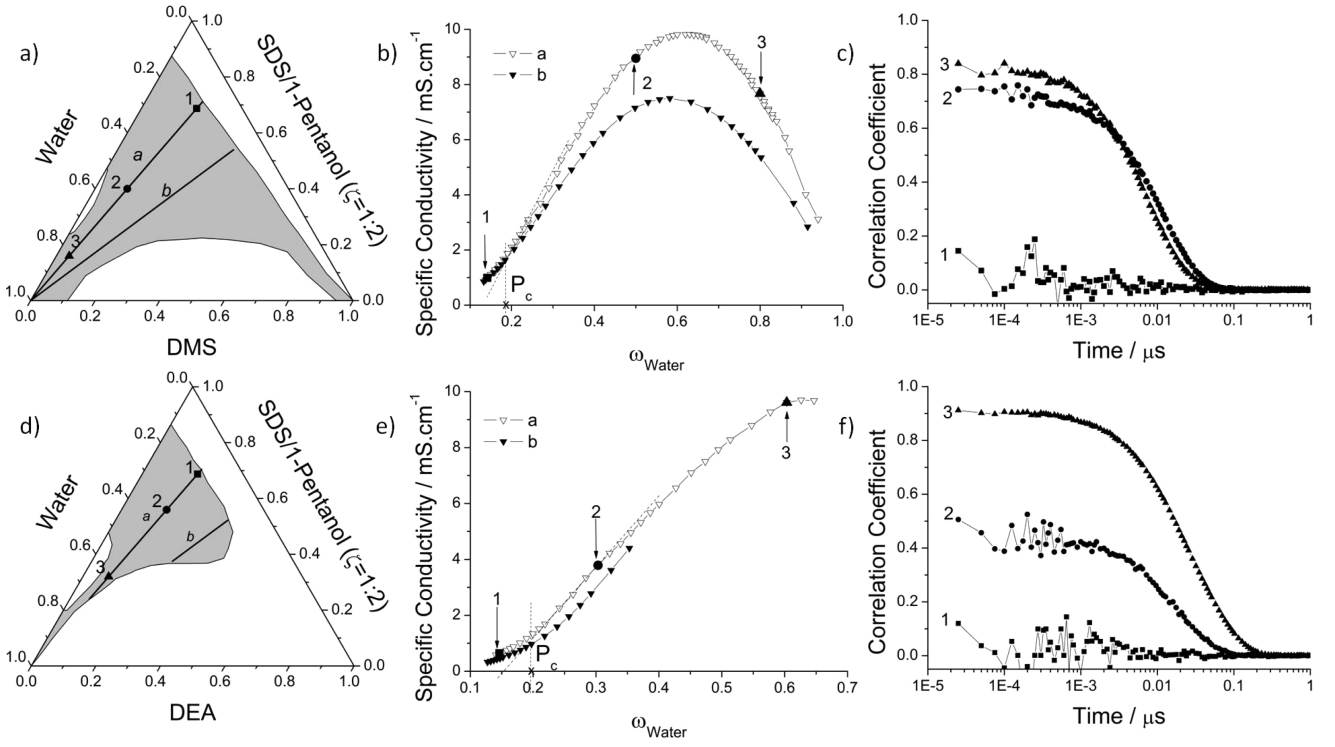

Figure 5. PTPDs obtained using (a) DMS and (d) DEA, respectively, as oils are shown in order to associate the topology of the realms of existence of the single phase to conductivity and DLS measurements. Paths *a* and *b* are the two lines where the conductivity experiments were performed (Figure 1). The three different points located on path *a* are the three corresponding compositions investigated with DLS. Curves (b) and (e) show the results of conductivity measurements following path *a* (▼) and b (∇). P_c is the percolation threshold. The three arrows give the compositions investigated by DLS. Curves (c) and (f) show the correlation functions obtained by DLS measurements for the three points. The symbols of the DLS curves correspond to the same symbols as shown in (a) and (d).

shown in Figure 4a, still a highly dilutable mE can be obtained, though the connection to the water-rich corner is diminished and only distinct dilution paths remain compared to Figure 3. None of these systems containing sodium oleate as surfactant are fully dilutable. Over 99 wt % of water, the solutions get a bluish appearance and turn turbid with time. This phenomenon had already been discussed in a previous work.[60] Figure 4b and c present systems with alternative nontoxic sustainable cosurfactants. After replacing 1-pentanol by ethanol or 1,5-pentanediol, no LC phases could be found. As a positive result, the area of highly water dilutable mE was increased, but the overall single-phase area for the system with 1,5-pentanediol was reduced. Using ethanol as cosurfactant had one striking disadvantage: high vapor pressure even at ambient temperature leads to a steady change in the composition, which leads to the risk of producing combustible emissions. The challenge was to find another nontoxic cosurfactant with comparable properties that is less hazardous. As discussed later, 1,5-pentanediol was a good choice for that. A drawback is the relatively high viscosity of the resulting mE in the oil- and surfactant-rich area, which is less pronounced in the water-rich region. It should also be mentioned that using sodium oleate had a significant drawback in combination with DBEs due to its high pK_a value. In the literature, the apparent pK_a value of oleic acid is reported to be between 8.0 and 8.5 by Cistola et al.[61] and 9.25 by Kanicky et al.[62] The resulting high pH will accelarate the hydrolysis of the diesters. The stability aspect of these systems is presented later.

Investigation of the Nanostructures of the Systems. In the next step, the nanostructures of the systems were investigated. Conductivity and DLS measurements were performed. In Figure 5, the results for the systems containing DMS and DEA are shown as examples because they are the most and least hydrophilic DBEs. Conductivity experiments were performed following paths *a* and *b* (Figure 5 a,d). The conductivity curves (Figure 5b,e) show always a percolative behavior. At very low water concentrations, the specific conductivity κ is almost zero. With increasing water content, κ starts slowly to increase until a linear correlation between the two parameters can be seen. From the extrapolation of the linear part of the curve, the so-called percolation point, P_c, can be derived. At a certain amount of water, the curve deviates again from linearity and reaches a maximum (slope = 0). With further increase of water, κ decreases. This behavior is linked to the different structures in the systems. For systems with hydrophobic DBEs, only the first part of the curves can be obtained due to the smaller area of mEs. The same evolution of κ can be seen for the systems with sodium oleate, ethanol, and 1,5-pentanediol. At water contents below P_c, the water molecules are bound to the surfactant headgroups, and a true solution is obtained. No defined structures can be observed in the systems by DLS measurements (Figure 5 c,f). Above this threshold, the structures in the systems become more pronounced with the addition of water as the evolution of the correlation functions shows. Now, enough water is in the system to form inverse micelles with a water core. This was observed for all investigated systems. Like in common percolative or U-type systems, the appearance of well-defined nanodroplets occurs when sufficient water is added to pass the percolation threshold P_c.

dx.doi.org/10.1021/sc300132x | ACS Sustainable Chem. Eng. 2013, 1, 603−610

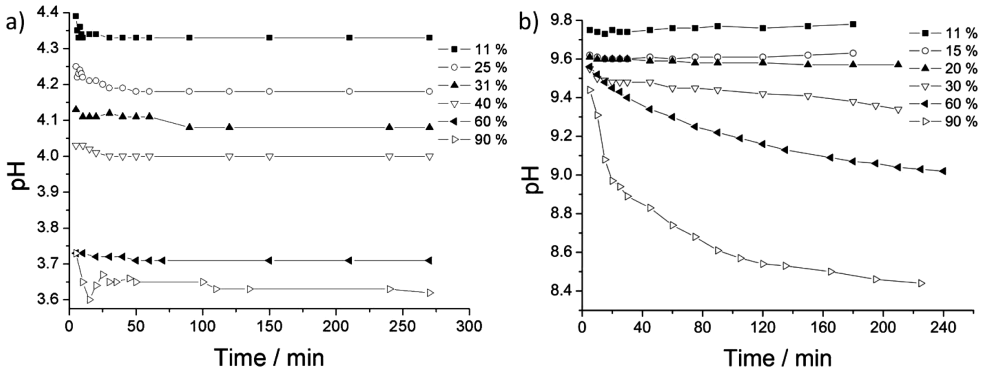

Figure 6. pH values as a function of time for the systems (a) water/SDS/1-pentanol/DMS and (b) water/sodium oleate/1-pentanol/DMS/DEA with $R_{DMS/DEA}$ = 3:2 and ζ = 1:2 at 25 °C. Every curve corresponds to one composition in the PTPDs. The percentages in the legends refer to the mass fraction of water in percent.

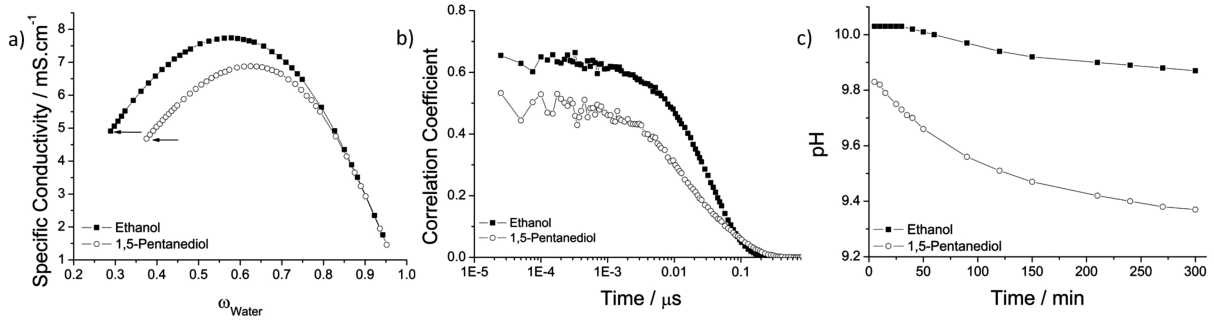

Figure 7. (a) Conductivity curves along path *a* of Figure 1 for the systems water/sodium oleate/ethanol ■ or 1,5-pentanediol ○/DMS/DEA with $R_{DMS/DEA}$ = 3:2. In these systems, no P_c is observed. The black arrows indicate the compositions studied with DLS (b) and where the pH stability (DBEs) was examined (c).

Stability Experiments. *Chemical Stability of DBEs in the Formulation.* To investigate the stability of the DBEs in the systems, we performed pH measurements. We are aware that the measured pH does not correspond to the real pH in the system, especially for samples with a very little amount of water. When we speak about the "pH", always the apparent pH is meant. The longtime stability of two systems, water/SDS/1-pentanol/DMS and water/sodium oleate/1-pentanol/DMS/DEA with $R_{DMS/DEA}$ = 3:2 and ζ = 1:2, is compared. The compositions correspond to the experimental path *a* shown in Figure 1. Figure 6 shows the evolution of the pH as a function of time for different water contents. For SDS samples, no significant change can be observed with time. The evolution of the pH value is linear, and the resulting solutions are acidic. Long chain fatty acids have a high pK_a, and so, as expected, the resulting aqueous solutions have relatively high pH values. So, systems with sodium oleate esters should be hydrolyzed very easily. From the curves in Figure 6b, it is obvious that for sodium oleate it has to be distinguished between two different regions. The pH value for samples with percentages of water $\leq P_c$, but still in the single-phase area, are remarkably stable. Formulations in the region of bicontinuous structures and direct mEs show a drop of pH value of several orders after a few minutes. An observation that can be made with the naked eye is the transition from a clear to a turbid solution after several days for samples with $\omega_{water} \geq 0.9$. So the conductivity, DLS, and pH experiments can be directly compared. The instability is linked to the formation of water nanodroplets and perhaps to the appearance of free water that is not completely bound by the surfactant ion pair. Nonstructured systems are stable in terms of hydrolysis, and these areas occur before P_c. At very distinct structures (pronounced correlation functions), the hydrolysis is more rapid.

In a further study, the stability of the two sustainable mEs with ethanol or 1,5-pentanediol were investigated. They show the same behavior as described above. Even samples with a very low amount of water show a significant drop of pH after short times. Comparing the conductivity and DLS measurements of these two systems, the same trend can be found concerning the formation of structures. In these two systems, no percolation thresholds can be detected, and significant correlation functions are obained by DLS for all water contents. The κ value is always increasing until reaching a maximum at high concentrations of water, which is not the case in an antipercolative system. This marks the point of phase inversion. It can be deduced that water nanodroplets exist from the beginning of the appearance of the single phase at low water content (Figure 7). The results show the possibility to formulate concentrated clear single-phase solutions that can evolve during an industrial process toward w/o, bicontinuous, and o/w mEs, adding water with a decelerated hydrolysis of DBEs in the starting formulation even at basic pH. The condition for this is the presence of a percolation threshold P_c and a quantity of water in the storage formulation below P_c. This is not the case using sodium oleate and ethanol or 1,5-pentanediol as cosurfactant. For these systems, fresh formulations have to be used in technical processes.

Volatile Stability of the Formulations. In the sustainable mEs, 1-pentanol was first replaced by ethanol. As described above, ethanol has a high vapor pressure even at room temperature, i.e., 5.760 kPa.[63] This is not only a problem because of the permanent change of the compositions during

evaporation but also because of the formation of dangerous flammable ethanol vapor. The flash point of ethanol is even less than ambient temperature (16−17 °C). To avoid this problem, 1,5-pentanediol is used in replacement, which has a very low vapor pressure, i.e., $5.5 \cdot 10^{-4}$ kPa.[64] For a better visualization of the evaporation, thermogravimetric (TG) measurements were performed. The mass of samples with the same compositions differing only by the cosurfactant (ethanol or 1,5-pentanediol) was recorded over 24 h at 32 °C. In Figure 8, the evolution of

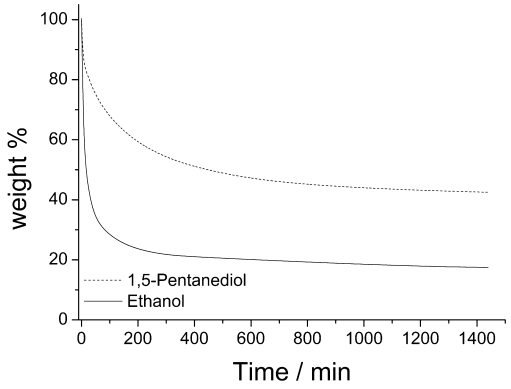

Figure 8. Loss of mass of single-phase formulations obtained with TGA at a constant temperature of 32 °C. The two samples have the same compositions except for the nature of the cosurfactant and are chosen to be on path *a* in Figure 1 with a water mass fraction of 0.4. The surfactant was sodium oleate, and the DBE was a melt of DMS and DEA with $R_{DMS/DEA}$ = 3:2.

the mass as function of time is shown. Subtracting the masses of water, DBE, and ethanol from the total mass corresponds to a loss of weight of 85%. This correlates very well with the 15% of total mass left in the sample derived from TG measurement. A different picture occurs for the system with 1,5-pentanediol. From the TG experiment, 40% of the original mass remains. The calculated loss of mass, assuming that only water and the DBE evaporate, is 44%. This value is again in good agreement with the experiment.

CONCLUSION

In this article, we show the possibility of formulating fully and highly water dilutable mEs with DBEs as a polar phase using SDS or sodium oleate as surfactant and 1-pentanol, ethanol, or 1,5-pentanediol as cosurfactant. Using SDS, the acidic pH prevents the degradation of the DBEs in the systems at any water content. In the presence of sodium oleate and 1-pentanol, the stability of DBEs is only favored at water concentrations lower than P_c. By contrast, an instability of the DBEs is observed even at the lowest possible water concentration to obtain single-phase areas in the systems water/sodium, oleate/ethanol, or 1,5-pentanediol/DBE. This instability can be linked to the nearly immediate formation of water nanodroplets. It can be inferred that a significant amount of free water molecules, i.e., not involved in hydration processes, drives the systems to the formation of water clusters responsible for the hydrolysis of the esters. On the other hand, the use of 1,5-pentanediol as cosurfactant gives a better thermical stability of the formulation because of its lower volatility compared to ethanol.

AUTHOR INFORMATION

Corresponding Author

*Fax: +49 941 943 4532. Tel: +49 941 943 4044. E-mail: werner.kunz@chemie.uni-regensburg.de.

Notes

The authors declare no competing financial interest.

ACKNOWLEDGMENTS

We thank Marco Dehling, Laura Egel, Daniel Wutz, and Josef Baumann for helping us with the experiments and Dr. Rainer Mueller for giving us access to his TGA apparatus.

REFERENCES

(1) Constable, D. J. C.; Curzons, A. D.; Cunningham, V. L. Metrics to 'green chemistry': Which are the best? *Green Chem.* **2002**, *4*, 521−527.
(2) Brands. Rhodia, Solvay, 2012. http://www.rhodia.com/en/markets_and_products/brands (accessed April 9, 2013).
(3) Gross, S. F.; Doerr, M.; Morris, T. C. U.S. Patent 20070093404 A1, 2007.
(4) Pabalan, R. T.; Aymes, C.; Graham, S.; Sehgal, A.; Trivedi, S.; Fluck, D.; Langlois, B. Patent WO 2011US01000 20110602, 2011.
(5) Fluck, D.; Sehgal, A.; Trivedi, S.; Pabalan, R. T.; Aymes, C. Patent WO 2011US01967, 2012.
(6) Kordosh, J. Patent WO 2011US45684 20110728, 2012.
(7) Frees, R. M.; Bortz, P. C. S. H. U.S. Patent 20070101902 A1, 2007.
(8) Machac, J. R.; Marquis, E. T.; Woodrum, S. A.; Darragas, K. Patent WO 2003062325 A2, 2003.
(9) S..Trivedi,; Fluck, D.; Sehgal, A. Patent WO 2011028274 A2, 2011.
(10) Wei, Y.; Cheng, F.; Li, H.; Yu, J. Synthesis and properties of polyurethane resins based on liquefied wood. *J. Appl. Polym. Sci.* **2004**, *92*, 351−356.
(11) Katz, H.; Iovino, C. A. Patent WO 2006108082 A2, 2006.
(12) Kaplan, W. A. Patent WO 2007092005 A1, 2007.
(13) Katrib, Y.; Calvé, S. L.; Mirabel, P. Uptake measurements of dibasic esters by water droplets and determination of their Henry's law constants. *J. Phys. Chem. A* **2003**, *107*, 11433−11439.
(14) Cukalovic, A.; Stevens, C. V. Feasibility of production methods for succinic acid derivatives: A marriage of renewable resources and chemical technology. *Biofuel Bioprod. Biores.* **2008**, *2*, 505−529.
(15) Zeikus, J. G.; Jain, M. K.; Elankovan, P. Biotechnology of succinic acid production and markets for derived industrial products. *Appl. Microbiol. Biotechnol.* **1999**, *51*, 545−552.
(16) Bechthold, I.; Bretz, K.; Kabasci, S.; Kopitzky, R.; Springer, A. Succinic acid: A new platform chemical for biobased polymers from renewable resources. *Chem. Eng. Technol.* **2008**, *31* (5), 647−654.
(17) Willke, T.; Vorlop, K. D. Industrial bioconversion of renewable resources as an alternative to conventional chemistry. *Appl. Microbiol. Biotechnol.* **2004**, *66*, 131−142.
(18) Song, H.; Lee, S. Y. Production of succinic acid by bacterial fermentation. *Enyzme Microb. Technol.* **2006**, *39*, 352−361.
(19) Rossi, C.; Hauber, J.; Singer, T. P. Mitochondrial and cytoplasmic enzymes for the reduction of fumarate to succinate in yeast. *Nature* **1964**, *204*, 167.
(20) Ling, E. T.; Dibble, J. T.; Houston, M. R.; Lockwood, L. B.; Elliott, L. P. Accumulation of 1-trans-2,3-epoxysuccinic acid and succinic acid by *Paecilomyces varioti*. *Appl. Environ. Microbiol.* **1978**, *35*, 1213−1215.
(21) Guettler, M. V.; Rumler, D.; Jaint, M. K. *Actinobacillus succinogenes* sp. nov., a novel succinic-acid-producing strain from the bovine rumen. *Int. J. Syst. Bacteriol.* **1999**, *49*, 207−216.
(22) Lee, P.; Lee, S.; Hong, S.; Chang, H. Batch and continuous cultures of *Mannheimia succiniciproducens* MBEL55E for the production of succinic acid from whey and corn steep liquor. *Bioprocess Biosyst. Eng.* **2003**, *26*, 63−67.

(23) chemicals-technology.com, 2012. http://www.chemicals-technology.com/projects/agro-industrie-plant/ (accessed April 11, 2013).
(24) Moss, C. W.; Kaltenbach, C. M. Production of glutaric acid. Useful criterion for differentiating *Pseudomonas diminuta* from *Pseudomonas vesiculare*. *Appl. Microbiol.* **1974**, *27* (2), 437−439.
(25) Draths, K. M.; Frost, J. W. Environmentally compatible synthesis of adipic acid from D-glucose. *J. Am. Chem. Soc.* **1994**, *116*, 399−400.
(26) CHEMSYSTEMS PERP Program, Report 08/09-2, February, 2010. http://www.chemsystems.com/reports/search/docs/abstracts/0809_2_abs.pdf (accessed April 9, 2013).
(27) Rennovia. http://www.rennovia.com/ (accessed April 11, 2013).
(28) Verdezyne Opens Pilot Plant To Produce Bio-Based Adipic Acid for Renewable 'Green' Nylon. Verdezyne. http://verdezyne.com/verdezyne/News/documents/VerdezynePilotPlantReleaseBusinessFINAL.pdf, 2012.
(29) Rico-Lattes, I.; Perez, E.; Franceschi-Messant, S.; Lattes, A. Organized molecular systems as reaction media. *C. R. Chim.* **2011**, *14* (7−8), 700−715.
(30) Schwuger, M.-J.; Stickdorn, K. Microemulsions in technical processes. *Chem. Rev.* **1995**, *95*, 849−864.
(31) Lindman, B.; Wennerstroem, H. Micelles. Amphiphile aggregation in aqueous solution. *Top. Curr. Chem.* **1980**, *87*, 1−83.
(32) Eicke, H. F. Surfactants in nonpolar solvents. Aggregation and micellization. *Top. Curr. Chem.* **1980**, *87*, 85−145.
(33) Do, L.; Withayyapayanon, A.; Harwell, J.; Sabatini, D. Environmentally friendly vegetable oil microemulsions using extended surfactants and linkers. *J. Surfactants Deterg.* **2009**, *12* (2), 91−99.
(34) Kahlweit, M.; et al. How to study microemulsions. *J. Colloid Interface Sci.* **1987**, *118* (2), 436−453.
(35) Chevalier, Y.; Zemb, T. The structure of micelles and microemulsions. *Rep. Prog. Phys.* **1990**, *53* (3), 279−371.
(36) Hoar, T. P.; Schulman, J. H. Transparent water-in-oil dispersions: The oleopathic hydro-micelle. *Nature* **1943**, *152*, 102−103.
(37) Anderson, J. L.; Ding, J.; Welton, T.; Armstrong, D. W. Characterizing ionic liquids on the basis of multiple solvation interactions. *J. Am. Chem. Soc.* **2002**, *124*, 14247−14254.
(38) Scriven, L. E. Equilibrium bicontinuous structure. *Nature* **1976**, *263*, 123−125.
(39) Langevin, D. Micelles and microemulsions. *Annu. Rev. Phys. Chem.* **1992**, *43*, 341−369.
(40) Lagues, M. Electrical conductivity of microemulsions: A case of stirred percolation. *J. Phys., Lett.* **1979**, *40* (14), 331−333.
(41) Lagourette, B.; Peyrelasse, J.; Boned, C.; Clausse, M. Percolative conduction in microemulsion type systems. *Nature* **1979**, *281*, 60−63.
(42) Zemb, T. *Colloids Surf., A* **1997**, *129*, 435−454.
(43) Eenam, D. N. V. U.S. Patent 5158710, 1992.
(44) Blum, R. L.; Robbins, M. H.; Hearn, L. M.; Nelson, S. L. U.S. Patent 5854187, 1998.
(45) Solans, C.; Kunieda, H., Eds.; *Microemulsions in Cosmetic, in Industrial Applications of Microemulsions*; Marcel Dekker: New York, 1997.
(46) von Rybinski, W.; Hloucha, M.; Johansson, I. Microemulsions in Cosmetics and Detergents. In *Microemulsions: Background, New Concepts, Application, Perspectives*; Stubenrauch, C., Ed.; John Wiley & Sons, Ltd: Chichester, 2009.
(47) Lawrence, M.; Rees, G. D. Microemulsion-based media as novel drug delivery systems. *Adv. Drug Delivery Rev.* **2000**, *45*, 89−121.
(48) Paul, B.; Moulik, S. P. Uses and applications of microemulsions. *Curr. Sci.* **2001**, *80*, 990−1001.
(49) Garti, N. Microemulsions as microreactors for food applications. *Curr. Opin. Colloid Interface Sci.* **2003**, *8*, 197−211.
(50) Garti, N.; Yaghmur, A.; Leser, M. E.; Clement, V.; Watzke, H. J. Improved oil solubilization in oil/water food grade microemulsions in the presence of polyols and ethanol. *J. Agric. Food Chem.* **2001**, *49*, 2552−2562.
(51) Rao, J.; McClements, D. J. Formation of flavor oil microemulsions, nanoemulsions and emulsions: influence of composition and preparation method. *J. Agric. Food Chem.* **2011**, *59*, 5026−5035.
(52) Papadimitriou, V.; Pispas, S.; Syriou, S.; Pournara, A.; Zoumpanioti, M.; Sotiroudis, T. G.; Xenakis, A. Biocompatible microemulsions based on limonene: Formulation, structure, and applications. *Langmuir* **2008**, *24*, 3380−3386.
(53) Ewbank, E.; Tummers, D. U.S. Patent 6.620.437B2, 2001.
(54) Accelerating Industry Innovation, 2012 Ethanol Industry Outlook. Renewable Fuels Association (RFA). http://ethanolrfa.3cdn.net/d4ad995ffb7ae8fbfe_1vm62ypzd.pdf (accessed April 9, 2013).
(55) Werle, P.; Morawietz, M. Alcohols, Polyhydric. In *Ullmann's Encyclopedia of Industrial Chemistry*; Elvers, B., Ed.; Wiley-VCH: Weinheim, 2002.
(56) Kaufman, D.; Reeve, W. 1,5-Pentanediol. *Org. Synth.* **1946**, *26*, 83−85.
(57) Xu, W.; Wang, H.; Liu, X.; Ren, J.; Wang, Y.; Lu, G. Direct catalytic conversion of furfural to 1,5-pentanediol by hydrogenolysis of the furan ring under mild conditions over Pt/Co_2AlO_4 catalyst. *Chem. Commun.* **2011**, *47*, 3924−3926.
(58) Clausse, M.; Nicolas-Morgantini, L.; Zradba, A.; Touraud, D. In *Surfactant Science Series, Microemulsion Systems*; Rosano, H. L., Clausse, M., Eds.; Dekker: New York, 1987.
(59) Klossek, M. L.; Touraud, D.; Kunz, W. Microemulsions with renewable feedstock oils. *Green Chem.* **2012**, *14*, 2017−2023.
(60) Klossek, M. L.; Marcus, J.; Touraud, D.; Kunz, W. Highly water dilutable green microemulsions. *Colloids Surf., A* **2013**, DOI: 10.1016/j.colsurfa.2012.12.061.
(61) Cistola, D. P.; Hamilton, J. A.; Jackson, D.; Small, D. M. Ionization and phase behavior of fatty acids in water: Application of the Gibbs phase rule. *Biochemistry* **1988**, *27* (6), 1881−1888.
(62) Kinecky, J. R.; Shah, D. O. Effect of degree, type, and position of unsaturation on the pKa of long-chain fatty acids. *J. Colloid Interface Sci.* **2002**, *256*, 201−207.
(63) Vapor Pressure of Ethanol. DDBST, GmbH. http://www.ddbst.com/en/EED/PCP/VAP_C11.php (April 9, 2013).
(64) 1,5-Pentanediol. ChemSpider. http://www.chemspider.com/Chemical-Structure.13839441.html (April 9, 2013).